Distribution Agreement

In presenting this thesis or dissertation as a partial fulfillment of the requirements for an advanced degree from Emory University, I hereby grant to Emory University and its agents the non-exclusive license to archive, make accessible, and display my thesis or dissertation in whole or in part in all forms of media, now or hereafter known, including display on the world wide web. I understand that I may select some access restrictions as part of the online submission of this thesis or dissertation. I retain all ownership rights to the copyright of the thesis or dissertation. I also retain the right to use in future works (such as articles or books) all or part of this thesis or dissertation.

Signature:

_____ _____

[David E. Smolar] Date

Investigation and Modeling of Binding Modes of Novel Small-Molecule Nox2 Inhibitors

By

David E. Smolar
Master of Science

Chemistry

_____

Dennis Liotta, Ph.D.
Advisor

_____

Jim Snyder, Ph.D.
Advisor

_____

Dale Edmondson, Ph.D.
Committee Member

_____

Michael Heaven, Ph.D.
Committee Member

Accepted:

_____

Lisa A. Tedesco, Ph.D.
Dean of the James T. Laney School of Graduate Studies

_____

Date

Investigation and Modeling of Binding Modes of Novel Small-Molecule Nox2 Inhibitors

By

David E. Smolar
Bachelor of Science, Emory University 2007

Advisor: Dennis C. Liotta
Advisor: Jim P. Snyder

An abstract of
A thesis submitted to the Faculty of the James T. Laney School of Graduate Studies of Emory University in partial fulfillment of the requirements for the degree of Master of Sciences

2010

Abstract

Investigation and Modeling of Binding Modes of Novel Small-Molecule Nox2 Inhibitors

The NADPH Oxidase Nox2 and its homologues are to play a central role in the production of harmful reactive oxygen species (ROS). Overexpression of ROS is believed to be involved in the pathophysiology of a number of chronic and acute disease states affecting millions of people. The binding orientation and site of novel small-molecule Nox2 inhibitors, believed to bind to the Nox2 subunit $p47^{phox}$ to inhibit its association with $p22^{phox}$, was undertaken using GLIDE docking. A ligand orientation, with a hydrogen bond acceptor oriented towards the amine of Trp 263, was discovered along with a nearby hydrophobic occupation in a site previously occupied by proline residues of the PRR of $p22^{phox}$. A model of this interaction was created and applied to the virtual screening of molecular libraries.

By David E. Smolar

Investigation and Modeling of Binding Modes of Novel Small-Molecule Nox2 Inhibitors

By

David E. Smolar
Bachelor of Science, Emory University 2007

Advisor: Dennis C. Liotta
Advisor: Jim P. Snyder

A thesis submitted to the Faculty of the James T. Laney School of Graduate Studies of Emory University in partial fulfillment of the requirements for the degree of Master of Sciences

2010

Acknowledgements

This thesis would not have been possible without the collaboration, support and advice of the following people: Patrick Baldwin, Dr. Thota Ganesh, Serdar Kurtkaya, Dr. David Lambeth, Dr. Susan Smith, Dr. Aiming Sun, and Dr. Dr. Pahk Thepcharti. I would also like to thank my advisors, Dr. Dennis Liotta and Dr. Jim Snyder, for their advice and the wonderful opportunity to be a part of their research group.

Table of Contents

Introduction: 1

Background: 3

Unmet Medical Need: Physiological Importance of ROS and NADPH Oxidases 3

Structure of Nox2: 10

Introduction to drug-like properties: 15

Current Lead Scaffolds and Known Structure-Activity Relationship (SAR): 19

SAR Rationale for Concerns of Covalent Binding 26

Methodology: 28

Description of Docking Methodology, Glide Software and Scoring Functions: 28

Glide Docking: 33

Induced Fit Docking: 34

Virtual Screening of Molecular Libraries: 35

ROCS Searching: 37

Results and Discussion: 38

Model of Binding Orientation: 38

Predictive Studies of AS-99 Derivatives: 49

Molecular Library Screening: 52

ROCS Searching: 55

Conclusion: 56

References: 59

List of Figures

Figure 1: Inactive Nox2; courtesy of Susan M. E. Smith of Emory University 12

Figure 2: Activated Nox2; Courtesy of Susan M. E. Smith of Emory University 13

Figure 3: $p47^{phox}$-$p22^{phox}$ binding showing the protein recognition region of $p22^{phox}$ with the $p47^{phox}$ dual SH3 domain receptor 15

Figure 4: Structure of sulfur scaffold and ebselen 20

Figure 5: Structure of the oxazole containing ligand TG4-225-2. 20

Figure 6: Dose response curve for TG4-225-2 21

Figure 7: Inactive compounds with substitution at the sulfur position 21

Figure 8: Compounds with opened thiazole ring 22

Figure 9: Compounds with methylene dioxy, ester or nitro substituents 22

Figure 10: JM3-77C, 87B & 87C 23

Figure 11: FP dose-response curves for JM3- 77C, 87B & 87C 23

Figure 12: Structure of AS-99 24

Figure 13*: Structures of AS-108 & AS-109* 24

Figure 14: Nucleophilic opening of the thiazol ring 27

Figure 15: Summary of SAR data relating to susceptibility to nucleophilic attack 27

Figure 16: Representation of favored docking pose (JM3-77C docked in $p47^{phox}$) 39

Figure 17: Top docked pose of JM3-53 in $p47^{phox}$ 40

Figure 18: Second favored pose of JM3-53 in $p47^{phox}$ 40

Figure 19: Docked pose of TG4 225-2 in $p47^{phox}$ 41

Figure 20: TG4-140 docked in $p47^{phox}$ 41

Figure 21: JM3-77C docked in $p47^{phox}$ 42

Figure 22: JM3-77C docked orientation shown with $P22^{phox}$ 43

Figure 23: JM3-87B docked in $p47^{phox}$ 44

Figure 24: JM3-87C docked in $p47^{phox}$ 45

Figure 25: AS-99 docked in p47^{phox} 45

Figure 26: AS-99 docked orientation shown with p22^{phox} 46

Figure 27: AS-109 docked in p47^{phox} 46

Figure 28: AS-108 docked in p47^{phox} 47

Figure 29: AS-99 scaffold derivatives for predictive studies 50

Figure 30: Ethyl substitution at R_1 in 1 51

Figure 31: Proline mimetic at R_1 in number 4 52

Figure 32*: Diels-Alder adduct in number 2* 52

Figure 33: *Representative hits from virtual screening of Chembridge Library* 54

Figure 34: Representative hits from ROCS searching 56

List of Tables

Table 1: IC_{50} values and docking scores 48

Introduction:

The selective inhibition of reactive oxygen species (ROS) producing NADPH Oxidases is a desirable medicinal chemistry target because reactive oxygen species produced by over-activated NADPH Oxidase is toxic to cellular components and have been implicated in a number of multiple disease states. Over-activation of NADPH Oxidases has been shown to play a role in the pathology of several chronic and acute disease states affecting millions of people. Antioxidant therapy, though it can target the downstream effects of ROS, represents a stoichiometric approach whose effect is largely negated by the large amount of ROS produced by NADPH Oxidases. Currently, no clinically viable therapeutic agent exists that is able to selectively inhibit NADPH Oxidase activity. The inhibition of these enzymes is therefore a desirable target for small-molecule drug development.

High-throughput screening, conducted by Emory's Molecular Libraries Screening Center Network (MLSCN) and synthetic optimization by the Emory Institute for Drug Discovery and Design (EIDD) in collaboration with the Lambeth group of Emory University, has identified a class of ligands believed to bind to the cytosolic Nox2 subunit $p47^{phox}$, inhibiting activity of the NADPH Oxidase Nox2. It is postulated that the reversible binding of the ligand to $p47^{phox}$ at the $p22^{phox}$ binding site is crucial to inhibitory activity. Currently, the exact enzyme binding site and mechanism of action of the inhibitory ligands is poorly understood. Alternative binding mechanisms, specifically the covalent or allosteric binding of the ligand to $p47^{phox}$, are suspected. Investigation and modeling of the

interactions between known active and inactive ligands and the active site is undertaken to elucidate a better understanding of the structure-activity relationship and lead optimization. The information obtained from this model can be leveraged for the virtual screening of large libraries of commercially available drug-like compounds to select molecules likely to have a favorable interaction with the $p47^{phox}$ binding site. The current goals of this project include the creation of both a potent inhibitor for use as a probe in biological studies and a viable drug candidate. Glide docking software is applied to investigate the geometry and mechanism of action between small-molecule Nox2 inhibitors and $p47^{phox}$.

Obtaining a qualitative and visual understanding of the ligand-receptor interaction allows for predictive structure-activity relationships, scaffold-hopping, and optimization towards a lead scaffold. Alternative and nonspecific binding mechanisms, which would not be accounted for using molecular mechanics docking software, were also studied. It is hypothesized that the inhibitors of the ebselen series bind at the $p22^{phox}$ binding site of $p47^{phox}$ with the following binding mode and interactions: orientation of the ligand in a manner in which the carbonyl is oriented towards Trp 263 or a homologous SH3 residue, an orientation favoring hydrogen bonding with Trp 263 with the chalcogen of the thiazole or selenazole ring oriented towards Met278. A hydrophobic interaction in the region surrounded by Pro 206, Gly 192, Asp 206 and Met 278 corresponding to the binding site of the proline residues of the $p22^{phox}$ protein is believed to be essential to successful ligand binding

To investigate this hypothesis, Glide docking and induced fit docking were applied to test the hypothesis that the active ligands bind non-covalently at the $p22^{phox}$ binding site on the $p47^{phox}$ protein. Attempts were made to utilize ROCS, Rapid Overlay of Chemical Structures, a method to identify compounds with similar 3-D structures and to perceive new scaffolds with similar activity. The identified binding motif was used to create constraints allowing for efficient screening of large molecular libraries using Glide High Throughput Virtual Screening and Glide Standard Precision.

Background:

Unmet Medical Need: Physiological Importance of ROS and NADPH Oxidases

As ROS production is a suspected or documented pathway behind a number of diseases affecting large segments of society, the development of a drug to selectively inhibit Nox represents a significant unmet medical need and desirable drug target. NADPH Oxidase produced superoxide results in a number of biologically active byproducts resulting in a wide range of physiological effects. Though Nox enzymes have been implicated in a large number of diseases affecting a wide range of systems, the physiological role of Nox enzymes and ROS has only recently become well understood and documented.

Superoxide produced by NADPH Oxidase has the ability to react *in-vivo* to create a number of promiscuously active compounds whose production can result in a wide range of physiological effects. In the presence of superoxide

dismutase, superoxide can produce hydrogen peroxide in the dismutation reaction shown below:

$$2O_2^- + 2H^+ \rightarrow H_2O_2 + O_2$$

Hydrogen peroxide itself has the ability to intercalate DNA, has a documented role in cell proliferation and anti-apoptosis, and is broken down in the presence of Iron(II) to produce the reactive hydroxyl radical in the following reaction:

$$H_2O_2 + Fe^{2+} \rightarrow OH^{\cdot} + OH^- + Fe^{3+} \qquad [1,4]$$

The hydroxyl radical participates in a large number of non-specific interactions, serves as a free radical initiator for radical polymerization, and is believed to have a large range of harmful or cytotoxic effects. In the presence of chloride ions and myleoperoxidase, hydrogen peroxide can react to form hypochlorite, the active ingredient in household bleach, in the reaction shown below:

$$Cl^- + H_2O_2 \rightarrow OCl^- + H_2O \qquad [1,4]$$

Hypochlorite can easily react with hydrogen peroxide to produce singlet oxygen, $^{1D}O_2$ as shown below:

$$H_2O_2 + OCl^- \rightarrow {}^{1D}O_2 + H_2O + Cl^- \qquad [1,4]$$

The product of this reaction, singlet oxygen, is often referred to as the reagent of last resort due to its wide reactivity and non-specificity. The harmful effects of singlet oxygen are broad, and it is likely that this species plays the largest role in the killing invading microbes in Nox2's role in phagocyte immune defense. The toxic nature of the byproducts from superoxide production underscores the

importance of inhibiting over-activated NADPH Oxidases to prevent harmful biological effects.

Historically the presence of reactive and often destructive reactive oxygen species was assumed to be an unfortunate byproduct of aerobic cellular energy generation through the Krebs Cycle. The presence of enzymes and other cellular mechanisms, namely peroxidase and superoxide dismutase to remove ROS, reinforced the view of ROS production as accidental. This long-held view first began to change as ROS produced by NADPH Oxidase enzymes was shown to play an integral role in the oxidative burst component of white blood cells' immune response. Phagocytes, namely neutrophils and macrophages, have been shown to express large amounts of Nox2. As their role in cellular defense was the first known and documented role, Nox enzymes were first referred to as oxygen burst enzymes. ROS produced by Nox2 participates in immune defenses through the non-selective oxidation of invading microbes and other invading biomolecules. The importance of Nox-produced ROS is well evidenced by conditions resulting in the knockout of ROS producing NADPH Oxidases, where decreased ROS production leads to compromised immunity. [1, 2, 3, 16]

One key piece of evidence in understanding the immunological role of ROS results from genetic conditions involving defects preventing the expression of ROS- producing enzymes. An illustrative example is patients suffering from chronic granulomatis disease, a condition first reported by Berendes in 1957 as a fatal childhood granulomatis condition. Children with chronic granulomatis

possess a genetic defect that blocks expression of the Nox2 subunits, preventing Nox2 activity and ROS production [5]. This is expressed as a defect in the white blood cells' ability to participate in oxidative burst and a severely compromised immune system. Unable to manufacture ROS, chronic granulomatis patients are highly susceptible to infection, abscess formation and must be treated with prophylactic antibiotics and antifungal agents. Though it is no longer reported as a fatal condition, the severity of this condition is illustrated by a long-term study conducted by Kobayashi *et al.* that followed twenty-three patients suffering from chronic granulomatis disease. This fifteen-year long study of patients lacking Nox2 activity showed an 87% survival rate and an average of one severe infection requiring hospitalization every five years, underscoring the central role of Nox2 in the body's immune defense [38]. Through clinical studies, genetic knockout studies, and examination of infected tissue for Nox2 and ROS concentrations, the role of NOX enzymes, and specifically the Nox2 isoform in the body's endogenous immune response, has been well documented and understood. As Nox enzymes play a crucial role in the body's immune defenses, a key concern for successfully and selectively inhibiting Nox enzymes remains immune suppression. [1, 2, 3]

More recently, NADPH Oxidases have been shown to have roles outside of immune response and, in fact, act as signaling molecules in the regulation of several physiological processes. Mutational and tissue analysis studies have shown that over-expression or over-activation of NADPH Oxidases plays a dominant role in the pathology of several diseases. Within the last decade, a

diverse family of NADPH Oxidase enzymes has been discovered. These NADPH Oxidases contribute to the in-vivo creation of reactive oxygen species. In contrast to the previous view of ROS existing as a byproduct of aerobic respiration, reactive oxygen species generated by NADPH Oxidase enzymes have been shown to play a significant role in cellular signaling. Over-activation of NADPH Oxidases has been implicated in a number of chronic and acute disease states. Disorders associated with over activated ROS generating enzymes includes fibrotic diseases, emphysema, inflammatory diseases, acute respiratory distress syndrome, atherosclerosis, ischemia-reperfusion injury, rheumatoid arthritis, type II diabetes and carcinogensis. With a dichotomy of roles such as immune defense, differentiation, signaling, and well as the production biological toxins leading to chronic disease later in life, the function of NADPH Oxidases has been described by David Lambeth of Emory University, as “a case of antagonist pleiotropy,” a a situation in which a desirable trait necessary for growth, survival, and reproduction causes harm later in life. Though they are essential signaling elements and immune molecules as we grow and reproduce, NADPH Oxidase-produced ROS often lead to aging, disease, and cancer later in life resulting an untimely death. [1, 2, 3, 4, 16, 20, 39]

A high level of Nox expression in the lungs is important for endogenous immune defenses, making the lungs especially susceptible to conditions involving the up-regulation of Nox enzymes and the subsequent over-expression of ROS. Nox-produced ROS has been implicated in the death of alveolar cells leading to the development of emphysema, while cigarette smoke and its

byproducts have been shown to up-regulate the Nox1 NADPH Oxidase isoform. Superoxide-derived hydrogen peroxide has been shown to be able to intercalate Tyrosine residues in extracellular matrix leading to fibrotic lung disease. Inflammation and tissue destruction related to asthma have been linked to an oxidant imbalance in the lung, while inflammation in airway has been linked to Nox2 [4,20]. Although not a direct result of non-specific ROS reactivity, over-activation of Nox dependant smooth muscle signaling has shown a link to pulmonary hypertension, which is often expressed as a condition related to cardiovascular disease development. [4, 13, 20]

One of the most pressing arguments for the development of selective NADPH Oxidase inhibitors is the implication of ROS in the pathogenesis of type II diabetes, a disease affecting 7.8% of the American population. According to the National Institutes of Health, a further 57 million Americans have “pre-diabetes” and are at risk for the development of type II diabetes. Diabetes results in direct medical costs of over $100 billion annually, results in over 70,000 non-traumatic amputations annually, and is the seventh leading cause of death in the United States. Ninety-five percent of diabetes patients suffer from type II diabetes [15]. Although type II diabetes is typically viewed as a “lifestyle disease,” the current understanding of this condition indicates that Nox inhibitors can play a role in the prevention of type II diabetes. A drug that could treat a fraction of people at risk for type II diabetes would represent a significant victory for preventative medicine. With over 57 million Americans at risk for type II diabetes, a tremendous potential market exists for Nox inhibitors, increasing the

likelihood that a viable Nox blocker would receive the funding and support in later stages of development. [15]

One of the main diseases associated with over-expression of ROS, cystic fibrosis disease, involves a compromise of the oxygen-dependant immune defenses of the airway. Current treatment for cystic fibrosis includes a significant prophylactic antibiotic regimen and antimicrobial treatments. Selective inhibition of the Nox isoform responsible for cystic fibrosis could provide an effective treatment for patients with this condition. [1, 2, 4, 13, 20]

Nox produced ROS has been shown to participate in the development of cardiovascular disease through many pathways. The signaling molecule NO, which is responsible for vasorelaxation, can undergo the following reaction with superoxide derived hydrogen peroxide to limit the availability of NO:

$$H_2O_2 + NO \rightarrow HONO + OH$$

Li *et al.* demonstrated that Nox2 over-activation in endothelial cells is increased by angiotension II, showing that this enzyme plays a role in the development of arteriosclerosis and cardiovascular disease through the angiotensin feedback pathway. [16] The ability of a NADPH Oxidase inhibitor to prevent vascular enodthelial cell hardening, interference with NO signaling, and cardiac cell damage would give physicians a desperately needed tool in the fight to prevent cardiovascular disease. [16]

Through extensive genetic knockout and loss of function mutational studies, NADPH Oxidase enzymes were discovered to be the predominant

source of in-vivo ROS. These oxides were discovered to be the byproduct of superoxide production by NADPH Oxidases. Furthermore, seven isoforms ROS generating NADPH Oxidases were discovered: Nox1, Nox2, Nox3, Nox4 Nox5, Duox1, & Duox2. These enzymes differ in their subunit requirement, mechanism of activation and tissue distribution. The large amount of ROS produced by dedicated NADPH Oxidases prevents the successful use of a stoichiometric antioxidant therapy, indicating that the most viable treatment for ROS related disorders is the selective inhibition of ROS production. [2, 3, 4, 5]

Structure of Nox2:

The NADPH Oxidase Nox 2 is an autoregulated transmembrane protein containing the $p22^{phox}$, $gp91^{phox}$ regulatory subunits in the b_{558} membrane bound cytochrome as well as the GTPase RAC and the cytosolic $p47^{phox}$, $p60^{phox}$, and $p40^{phox}$ subunits. Activation of Nox2 requires the association between the cytosolic components, $p47^{phox}$, $p60^{phox}$, $p40^{phox}$ and the $p22^{phox}$ of the membrane-bound flavocytochrome. Activation of Nox 1, 2 & 3 occurs via a mechanism similar to that of Nox1 & Nox3, while Nox4-5 and Duox 1-2 are activated through a calcium dependant pathway. [2,5]

In order to bind to $p22^{phox}$, serine residues on the polybasic region of the C-terminal of $p47^{phox}$ must first be phosphorylated. This opens the dual SH3, or Bis-SH3 domain for $p22^{phox}$ binding allowing for Nox2 protein assembly and catalytic activity. Activation can result from a cellular stimulus such as inflammation. The phosphorylation of serine residues, including Ser-303, Ser-

304, and Ser-328 are necessary for the unmasking of the SH3 domain on $p47^{phox}$, although it has been shown that nearly all serines on the polybasic region are typically phosphorylated for activation of the SH3 domains. [5,30] The protein recognition region of the C-terminal of $p47^{phox}$ consists of a proline rich region that binds to the SH3 domain. Upon phosophorylation, the BIS-SH3 domain opens up and is available for binding with the membrane bound $p22^{phox}$. A complex of cytosolic $p67^{phox}$, $p40^{phox}$ and phosphorylated $p47^{phox}$ translocates to the membrane bound $p22^{phox}$, forming the Nox2 cytochrome.

Concurrently, the GTP binding cytosolic RAS protein translocates to the membrane to bind to the Nox2 complex. Successful binding between $p22^{phox}$ and $p47^{phox}$ is necessary for activation of the enzyme and ROS production. Upon assembly, catalytic activation occurs and superoxide is produced from NADPH Oxidase in the following reaction:[2,5]

$$2O_2 + NADPH \rightarrow 2O_2^- + NADPH^+ + H^+$$

NADPH Oxidase facilitates the transfer of electrons from NADPH to molecular oxygen. The activation of these subunits is shown in the following schematic, courtesy of Susan M. E. Smith of Emory University:

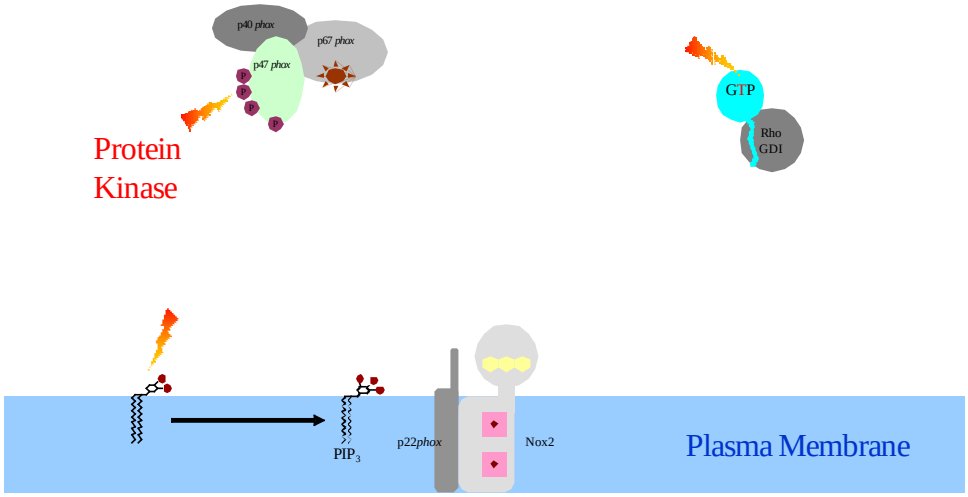

Figure 1: Inactive Nox2; courtesy of Susan M. E. Smith of Emory University

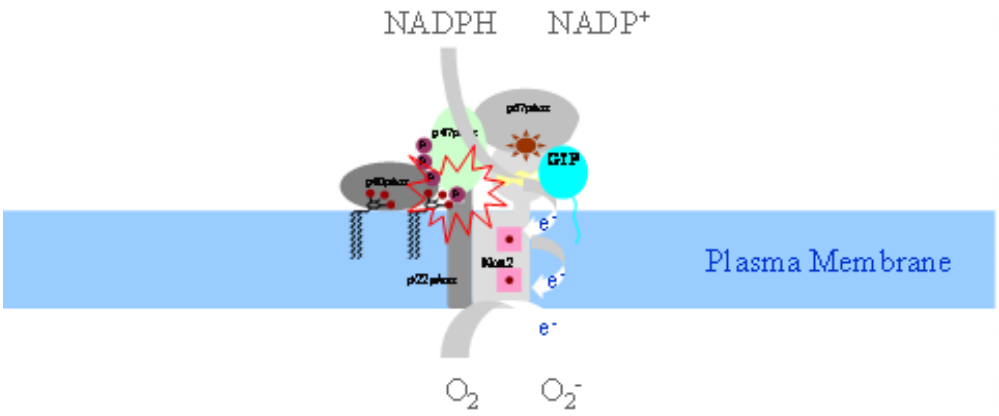

Figure 2: Activated Nox2; Courtesy of Susan M. E. Smith of Emory University

Blocking the assembly of Nox2 will inhibit enzyme activity and ROS production. For this reason, the assembly of the $p47^{phox}$ and $p22^{phox}$ cytosolic subunits has been targeted for small-molecule drug development. Groemping's 2003 characterization of Nox2 using X-ray crystallography revealed the structure of the Bis-SH3 domain with a collaborative binding grove for $p22^{phox}$ formed from the interface of the two SH3 domains. [2, 5] Lambeth *et al.* of Emory University developed an assay to measure the unbinding of a synthetic protein recognition region, PRR, of $p22^{phox}$ from a GST-tagged $p47^{phox}$. This synthetic PRR of $p22^{peptide}$ used in this assay is rhodamine labeled. Unbinding of $p22^{phox}$ results in the observed signal, polarization caused by unbound synthetic $p22^{phox}$. This assay allows for the efficient measurement of dose-response upon addition of an inhibitory ligand. A secondary assay, measuring the cell-free peroxide production, is utilized by Lambeth *et al.* to measure the dose-response of

inhibitory ligands. As the cell-free assay does not necessarily correlate directly with inhibition of $p47^{phox}$ –$p22^{phox}$ binding, small molecule inhibitory values from the fluorescence polarization assay will be used for the majority of this work.

Introduction to drug-like properties:

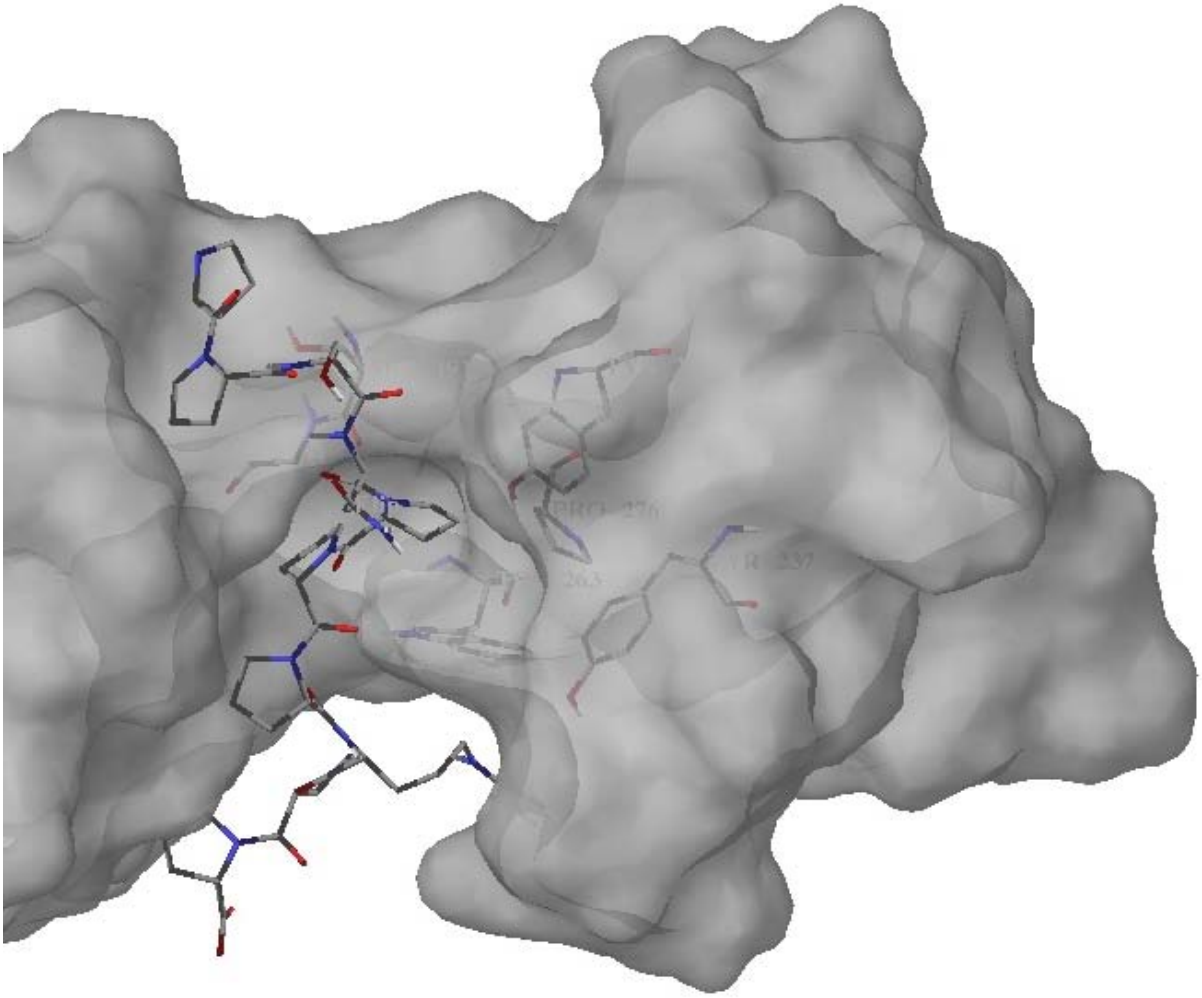

Figure 3: p47^{phox}-p22^{phox} binding showing the protein recognition region of p22^{phox} with the p47^{phox} dual SH3 domain receptor

The region surrounding the p22^{phox} binding site is a proline rich region and contains two tryptophan residues, Trp 193 & Trp 263. As shown in Figure 3, an image of p47^{phox}, the binding site of p22^{phox} is a shallow groove and lacks an obvious small-molecule binding pocket. Although ligands' binding to shallow

protein groves have the potential to act as inhibitors for a number of highly desirable drug targets, including numerous cancer signaling molecules in addition to Nox enzymes, the shallow grooves of protein-protein interactions typically represent one of the most difficult targets for rational drug design. [23,24,25,26,27] The dynamic nature of a shallow protein-protein interaction site, which is poorly represented in the time-averaged crystal structure, presents a number of challenges for computationally aided rational drug design. Far from ideal small-molecule drug targets, typically small deep pockets, protein-protein interactions typically involve a surface area of interaction often exceeding 1,000 $Å^2$. Physical properties suggested for an orally bioavailable drug as summarized in Lapinski's Rule of Five argue against the creation of molecules of the size required to fully occupy such a binding site. Lapinski's rules generally state that an orally available therapeutic will have no more than one violation of the following: a maximum of five hydrogen bond acceptors, no more than ten hydrogen bond donors, a molecular weight no greater than 500 and an octanol-water partition coefficient logP <5. Drugs meeting these requirements typically have acceptable absorption, distribution, metabolism and excretion (ADME) characteristics that allow for them to cross the hydrophobic intestinal lipid bilayer to be absorbed into the blood stream. [34,35] With an extremely large site occupied by a small ligand, a number of ligand binding poses[1] are possible for the inhibition of a large protein-protein interaction, as is the case for the $p22^{phox}$ binding site on $p47^{phox}$.

[1]**Pose:** the orientation and conformation of the ligand in the receptor

It has been shown in several instances that small-molecule inhibition of protein-protein interactions can occur through a number of mechanisms that bypass what would be typical competitive interactions at the protein-protein interaction site. The allosteric binding of regulatory small molecules, namely Lovastatin, was shown to block the binding of leukocyte function-associated antigen-1 (LFA-1) to its endothelial-cell-ligand intercellular adhesion molecule-1 by inducing a structural modification in the receptor to inhibit protein-protein interaction. [26] A similar allosteric inhibitor motif was demonstrated to prevent the dimerization of inducible nitric oxide synthase (iNOS). [26] Kessl *et al.* demonstrated the ability for a small-molecule to inhibit protein-protein interactions in HIV-1 integrase, an enzyme that inserts viral RNA into the host chromosome using an allosteric mechanism.[29] Although the large size of the protein-protein interaction may be contraindicative to allosteric ligand binding, these examples clearly demonstrate the ability of allosterically bound small-molecule inhibitors to induce a significant structural change and thereby prevent a successful protein-protein interaction. [26,27,29]

If an obvious small-molecule drug-like pocket is not observed for a given protein, the possibility of a transient druggable pocket at the active site opening in a dynamic protein system should still be considered as a possible mode of binding for the series of ligands being considered. Eyrisch *et al.* used extensive molecular dynamics simulations to demonstrate the opening of small, transient, drug-like pockets on the surface of protein-protein interaction sites. It was demonstrated in 10 ns long molecular dynamics simulations that small pockets

opened and closed at the protein receptor site, remaining open for an average of 2.5 ns. In the case of $p47^{phox}$ the possibility of a pocket opening up and exposing a nucleophilic residue, for example the lone cystine on $p47^{phox}$ to attack the labile nitrogen-chalcogen bond of the thiazole like ring, should not be discounted *ex facie*. Though such an interaction may be considered improbable, the possibility of small-molecule Nox2 inhibitors binding at a location other than the $p22^{phox}$ binding site should be considered a possibility until additional evidence allows it to be confidently ruled out.

The currently available assays do not allow for appropriate investigation of whether the ligand binds at the p22 binding site. Although earlier mutational studies revealed the location of the amino acid residues needed for $p47^{phox}$-$p22^{phox}$ binding, it is not possible to conduct a study of ligand binding sites by mutating residues on the binding groove of $p47^{phox}$ with the current assays. Although mutation of residues responsible for binding the active ligand would likely interfere with the binding of this ligand to the protein, the mutation of these residues would prevent the binding of $p22^{phox}$ resulting in a false positive in the fluorescence polarization assay. In the cell-free assay, mutating residues responsible for binding $p22^{phox}$ would prevent the translocation of the $p47^{phox}$ complex to the membrane and thereby prevent any Nox2 activity.

Typically a simple enzyme kinetics study involving out-competing the ligand with excess substrate is able to test for competitive versus covalent or allosteric type interactions through introduction of an excess of substrate. In this case, with the $p22^{phox}$ peptide, the nature of the fluorescence polarization assay

does not allow for this test. In the fluorescence polarization dose-response assay, the displacement of a synthetic rhodamine labeled peptide corresponding to the protein recognition region of $p22^{phox}$ from a GST labeled Bis-SH3 domain of $p47^{phox}$ is tracked. Upon exit of the peptide from the Bis-SH3 domain, the increase polarization from unbound labeled $p22^{phox}$ is the recorded signal. Attempts to out-compete the ligand with an excess of labeled synthetic $p22^{phox}$ would result in a saturation of signal from the unbound peptide, and the binding of the ligand would not be discernable. Competitive inhibition, allosteric inhibition, or covalent binding at the active site could result in the observed assay results.

Current Lead Scaffolds and Known Structure-Activity Relationship (SAR):

High-throughput screening conducted by Emory's MLSCN, 2-D similarity searching, and synthetic derivatization by Emory's Institute for Drug Discovery and Design revealed a lead series of compounds with the basic scaffold shown in *figure 4.* Extensive synthetic work was conducted by Thota Ganesh, Jaeki Min and Aiming Sun of the EIDD to develop the Structure activity relationship (SAR) discussed in this section. Lambeth *et al.* developed and conducted the fluorescence polarization assays used to investigate the activity of these molecules against the Nox2 enzyme. This SAR data formed the starting point for the investigation of binding between Nox2 inhibitors and $p47^{phox}$. [12]

Figure 4: Structure of sulfur scaffold and ebselen

The IC_{50} values, measured by Lambeth *et al.* of the Emory University Department of Pathology, represent the ligand dose required for 50% inhibition and a measure of the ligand binding affinity to the target site. They are generally in the 0.3-10 μM range. The sulfur containing lead scaffold, 2-phenylbenzo[d]isothiazol-3(2H)-one shown in *figure 4*, has an FP IC_{50} of approximately 4.7 μM in the fluorescence polarization (FP) assay while ebselen shows a measured FP IC_{50} of around 0.3-0.7 μM. This demonstrates an approximately ten-fold improvement in activity upon replacement of sulfur with the heavier chalcogen selenium. Replacement of the thiazole ring with an oxazole ring, as in the case of TG4-225-2, *figure 5*, synthesized by Thota Ganesh and analyzed for FP activity, *figure 6,* by Lambeth *et al.,* demonstrates this loss of activity.

Figure 5: Structure of the oxazole containing ligand TG4-225-2.

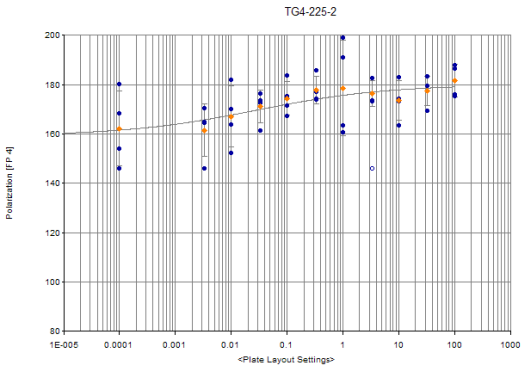

Figure 6: Dose response curve for TG4-225-2

Similar to the loss of activity encountered upon substitution of oxygen for a sulfur or selenium, activity is also lost upon replacement of the sulfur position with an amine, alkyl or sulfone. The non-active molecules, shown in *figure 7*, were synthesized by chemists at the EIDD and demonstrate the effect of these substitutions.

Figure 7: Inactive compounds with substitution at the sulfur position

Finally, activity is lost upon opening of the thiazole ring as shown by the compounds depicted in *figure 8.*

Figure 8: Compounds with opened thiazole ring

As demonstrated by the following compounds shown in *figure 9*, activity is significantly improved by substituting the benzene ring with a methylene dioxy, ester or nitro group.

Figure 9: Compounds with methylene dioxy, ester or nitro substituents

In summary, the thiazole or selenazole rings appear central to the activity of these scaffolds while the introduction of a hydrogen bond acceptor on the benzene ring appears to improve activity.

Structures in *figure 10* and the appropriate FP dose-response curves shown in *figure 11* demonstrate the SAR of different alkyl substitution on the ester. These compounds are studied in detail later in this work: [12]

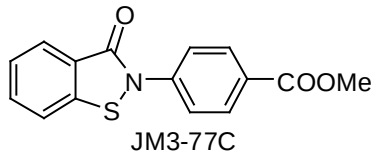

JM3-77C

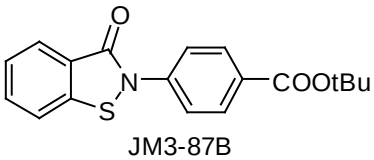

JM3-87B

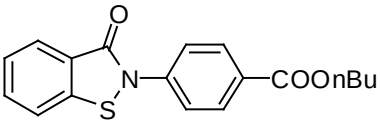

JM3-87C

Figure 10: JM3-77C, 87B & 87C

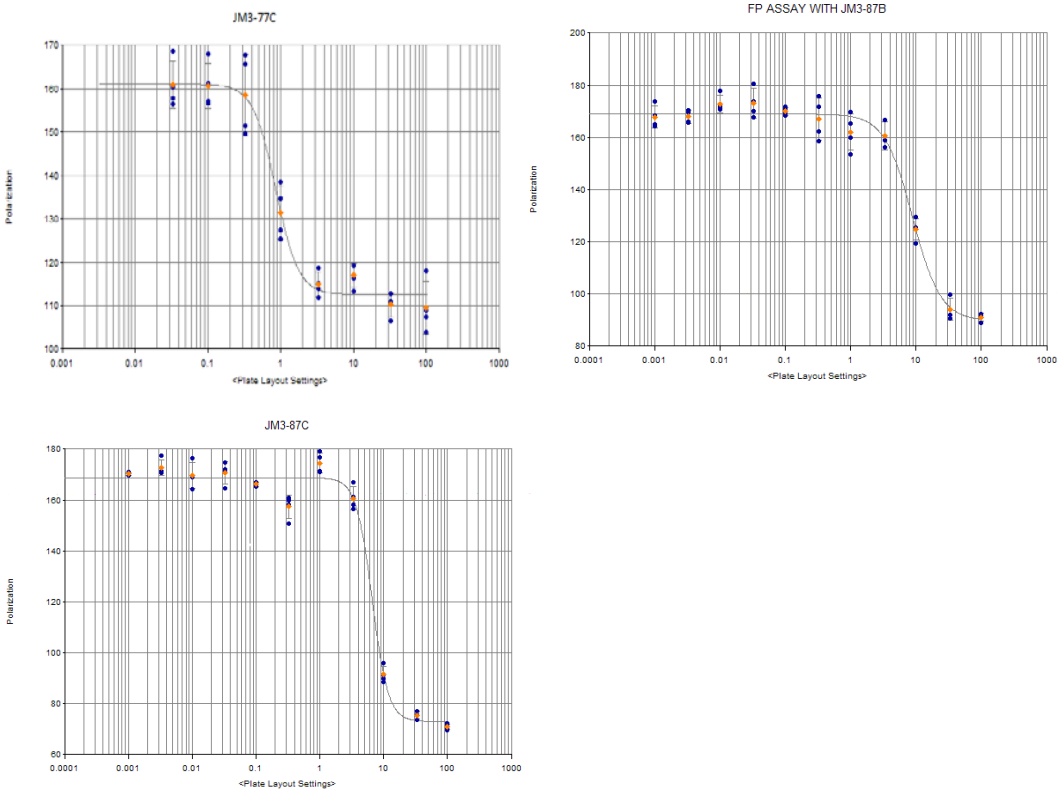

Figure 11: FP dose-response curves for JM3- 77C, 87B & 87C

As shown above in the FP dose-response curves, JM3-77C has an FP IC_{50} of 0.8 μM, JM3-87B 10 μM and JM3-87C 7μM. The difference in binding, as shown by Glide docking, for these three molecules is studied in this work and described below.

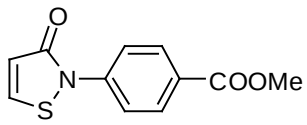

AS-99

Figure 12: Structure of AS-99

AS-99, *figure 12* above, is an uncharacteristically active small molecule given its inhibitory activity. AS-99 contains the characteristic thiazole ring and was shown to have a FP IC_{50} of 4.5 μM. The following derivative of AS-99, known as AS-108 and AS-109, *figure 14,* were shown to have no inhibitory activity in the FP assay. These compounds along with AS-109 were investigated in an attempt to ascertain a consistent binding mechanism for the active ligands.

Figure 13*: Structures of AS-108 & AS-109*

The structural feature common to all active ligands is the presence of a thiazole or selenazole ring, which appears to be central to activity of the ligands. Although compounds exhibiting this central structure have shown the greatest

promise as inhibitors of Nox2, they are not viewed favorably as candidates for drug development. These compounds are small, hydrophobic and likely toxic. In addition, similar compounds, and ebselen in particular, have been well documented in the literature, indicating significant prior art that may make these compounds economically non-attractive for further research and development.

A significant concern exists that these compounds participate in promiscuous covalent binding with nucleophilic amino acid residues. Ebselen has been documented by Ullrich *et al.* to participate in a reversible covalent binding with cystine residues. [22] The requirement for a labile nitrogen-chalcogen bond makes these compounds both promiscuous binders and good substrates for glutathione metabolism.

Though these scaffolds possess a number of seemingly problematic characteristics, evidence exists supporting the safety and efficacy of the compounds. Ebselen has been successfully used in humans for the treatment of acute ischemic stroke. [17, 18] Yamaguchi *et al.* conducted a phase II clinical trial treating ischemic stroke patients 300mg/d of oral ebselen. Treatment was begun within 24 hours of stroke and continued for two weeks post-stroke. Though ebselen's poor solubility prevented intravenous administration, a suspension was readily absorbed through the gastrointestinal tract. This trial indicated a significant improvement in ischemic stroke patients treated with ebselen at the one-month follow-up, although a three-month follow-up showed no statistically significant improvement for the 151 patients treated with ebselen versus 149 control patients. Most importantly, this clinical trial showed that

300mg/d PO was well tolerated over two months and resulted in no adverse side-effects at this dose. Yamaguchi's study also showed that a similar and even reduced rate of lung infection occurred in stroke patients treated with Ebselen versus control, indicating that the expected reduced immune function expected by lowering ROS in these patients did not occur. This may also have positive implications for the treatment of fibrotic diseases. [17, 18]

Though this scaffold has been successfully demonstrated in clinical trials, this does not necessarily indicate that this scaffold is a good candidate for a Nox inhibitor. The acceptable toxicity for a new chemical entity treating an acute and life-threatening condition is significantly different than that needed for long-term use. Although this compound may indeed be acceptable for the treatment of stroke, for transplant-related ischema-reperfusion injury and other acute conditions significantly more safety concerns exist when developing a compound for long-term use.

SAR Rationale for Concerns of Covalent Binding

The ability of the target ligand to accept a nucleophile and break the Nitrogen-Sulfur or nitrogen-selenium bond could not be ruled out through docking studies. Though mutagenic studies indicate the importance of the Trp193 for the binding of small-molecule ligands, the possibility remains that an allosteric interaction is responsible for the small-molecule binding. The following reaction between the lead ligand scaffold (shown below, *figure 14*) remains a concern:

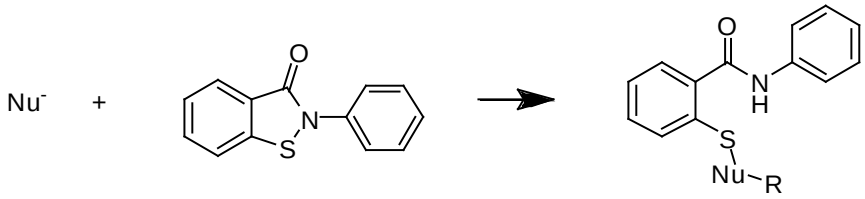

Figure 14: Nucleophilic opening of the thiazol ring

The general SAR, summarized in *figure 15,* reinforces the concern that covalent bonding via nucleophilic attack of the nitrogen-chalcogen occurs.

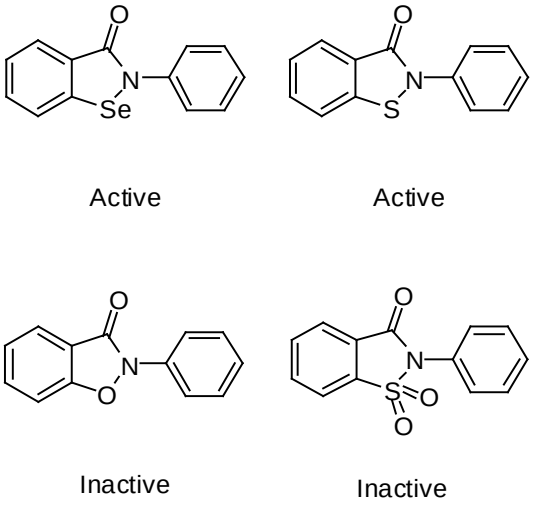

Figure 15: Summary of SAR data relating to susceptibility to nucleophilic attack

Replacement of sulfur with selenium, resulting in a more polar and reactive N-Se bond, increases activity by an order of magnitude. This concern is reinforced by the complete loss of activity that is observed upon replacement of sulfur with an atom less likely to undergo nucleophilic attack. While selenium significantly increases activity, all compounds tested with carbon, oxygen, or sulfones in place of sulfur showed a complete loss of activity. Such centers are well-known to be much poorer electrophiles.

The covalent binding of ebselen to thiol containing amino acid residues has been document by Ullrich *et al.* at the University of Konstanz [22]. This group utilized UV absorption spectroscopy to demonstrate a decrease in the characteristic 346nm absorbance of ebselen along with the appearance of a product band upon reaction of ebselen with albumin protein. This binding was further confirmed when ^{14}C labeled ebselen was observed to migrate with albumin protein on an SDS-gel. Interestingly, the author failed to detect a clear isosbestic point during the study followed by UV absorption, possibly indicating a non-specific or side reaction with other residues. The presence of an isosbestic point would indicate the presence of two species whose absorbance is equal at the isosbestic point. The presence of an isosbestic point indicates a one to one reaction. [22]

Methodology:

Description of Docking Methodology, Glide Software and Scoring Functions:

Schrodinger's Glide (Grid-Based Ligand Docking with Energetics) is a molecular docking program designed to investigate the multiple conformations of a ligand, identity conformations that best take advantage of the pharmacophoric features of a receptor site, and rank-order them with a parameterized scoring function and efficiently screen large virtual compound libraries by flexible ligand docking to a rigid receptor. Glide performs a positional, orientational, and conformational search of the ligand in the protein active site [6]. In its current form, this software offers several levels of precision for computation: high-

throughput virtual screening (HTVS), standard-precision (SP), and extra-precision (XP). These features allow an investigator to tailor the necessary computational level to his projects, depending on his need to either understand the interaction preferences of a handful of ligands to a target of interest or search through a large library of compounds to identify potential biological molecules.

To dock ligands, Glide first generates a grid over the receptor cavity and calculates the energy of interaction between the receptor and each possible ligand atom at every grid point. An energy grid, or potential energy gradient, is created in the receptor which is divided into smaller 0.3 $Å^3$ grids. Once each subgrid is parameterized and interaction energies are calculated a smoothing function applied to the receptor grid. This allows for treatment of the grid as a continuum. A conformational search of the likely conformations is performed on-the-fly for each ligand, creating a large number of possible conformations. Each of these is then docked into the pre-calculated grid and an interaction value is obtained using the Glide scoring function to rank order the generated poses. [6, 7, 8]

At the heart of the Glide software is its scoring function, which incorporates experimental measurements and energetic values for molecular and atomic interactions from a variety of protein-ligand interactions. The Glide scoring function is derived from that of Eldridge, with some corrections, and is based on the following equation:

$$\mathbf{\Delta G_{bind}} = C_{\text{lipophilic-lipophilic}}\,\Sigma f(r_{\text{lr}}) + C_{\text{hbond-neutral-neutral}}\Sigma g(\Delta r)h(\Delta\alpha) + C_{\text{hbond-neutral-charged}}(\Delta r)h(\Delta\alpha) + C_{\text{hbond-charged-charged}}(\Delta r)h(\Delta\alpha) + C_{\text{max-metal-ion}}\Sigma f(r_{\text{lm}}) + C_{\text{rot}}H_{rotb} + C_{\text{polar-hydrophobic}}V_{\text{polar-hydrophobic}} + C_{\text{coulombic}}E_{\text{coulombic}} + \text{solvation terms} \quad [6,8]$$

The above equation incorporates the known energetics of lipophilic interactions, hydrophobic interactions, hydrogen bonding, and metal interactions, while incorporating the scoring coefficients g, h, and r to scale these interactions based on the ligand-protein geometry. [6] For metal ligation, the most favorable ligation energy is chosen when several are possible. [6] Typically, for drug-like compounds, the lipophilic interaction energy is substantial and typically composes the most significant component of the Glide methodology. For the SP (standard precision) docking mode, the scoring function and energies of interaction are designed to provide a “softer” [6] function that is less likely to exclude false negatives by severely penalizing interactions violating established physical principles. As one goal of Glide is to screen large compound libraries, it is advantageous to employ scoring functions that allow the inclusion of false positives as they may be eliminated in subsequent biological screening.

By following the same general principles, the Glide XP scoring function incorporates extra terms for desolvation, entropy penalties, π-π stacking, and hydrophobic interactions as described by the following equation: [11]

$$\textbf{XP GlideScore} = E_{coul} + E_{vdW} + E_{bind} + E_{Penalty} \quad [11]$$

Where:

$$\textbf{E}_{\textbf{bind}} = E_{hyd\_enclosure} + E_{hbond\_neutral\text{-}neutral\_motif} + E_{hbond\_charged\text{-}charged\_motif} + E_{VI} + E_{hbond\_pair} + E_{phobic\_pair} \quad [11]$$

And:

$$\textbf{E}_{\textbf{penalty}} = E_{desolvation} + E_{ligand\ strain} \quad [11]$$

The Glide XP scoring function attempts to better incorporate the energy penalty suffered when water molecules are displaced from a hydrophobic protein region or around a hydrophobic ligand. This scoring function was originally correlated to binding affinity, achieved by parameterizing the interactions between the receptors and ligands with experimentally determined geometries of ligand-protein complexes and their binding and affinity values. Although it was parameterized against binding affinities, the software makes no claims that the determined scoring or interaction values directly correlate Glide Score and binding affinity.

The Schrodinger software packages allows researchers to rescore ligand poses using the Molecular Mechanics Generalized Born Solvent Accessible (MM-GB/SA) method. This relies on the following scoring function:

$$\textbf{}\Delta G\textbf{bind}_{\textbf{MM-GB/SA}} = \Delta E_{intramolecular} + \Delta G_{solvation} - T\Delta S_{conf} + E_{vdW} + E_{electrostatic} + E_{protein} \quad [44]$$

The main contribution of this scoring model is the inclusion of the terms $G_{\text{solvation}}$ and $E_{protein}$. $G_{solvation}$ allows for the extensive inclusion of salvation terms while final term, $E_{protein,}$ *is* a measure of the strain on the protein caused by the presence of the ligand. MM-GB/SA scoring typically favors lipophilic interactions over hydrogen bonding interactions. [44] In the binding of small molecules to protein receptors, it is reasoned that that non-polar interactions are primarily responsible for the binding between drugs and the protein because hydrogen bonding sites will be occupied whether the receptor is occupied by either solvent or water. In many studies, MM-GB/SA has been shown to have superior performance over Glide scoring functions when predicting ligand-receptor interactions. [44]

Glide docking of ligands into a target protein generates docked poses, various ligand orientations and conformations in the receptor. The quality of the interactions, the ability of the ligand to deviate slightly from the most favorable pose and scoring function must be taken into account when interpreting these poses. In the present work, docking runs were set to generate a maximum of 50 poses per ligand. The generation and recurrence of a type of pose within the generated results may indicate a favorable binding pattern. The quality of the docking was judged based on the models' ability to account for the biological activity of the ligands and correlation with known interactions with the receptor. For these reasons, the analysis of the docked poses is ultimately qualitative in nature.

Known interactions between the protein and ligand can be included for constrained docking, requiring certain parameters such as the occupation of a certain region by a hydrophobic group, hydrogen bonding with specific atoms, or the occupation of a region with a specific group. These constraints significantly reduce the degrees of freedom necessary for docking and therefore significantly reduce the amount of time necessary for screening large libraries of compounds. Once a favorable ligand-receptor interaction model has been established, it is proposed to use the receptor model to screen large libraries of compounds with the goal of discovering new Nox2 inhibitors.

Glide Docking:

The crystal structure of the $p47^{phox}$-p22 complex, known as 1OV3, obtained by Groemping at a resolution of 1.8 Angstroms was obtained from the Protein Data Base (PDB). [5, 40] This structure was preprocessed to assign bond orders, add missing hydrogens and ensure chemically reasonable bond lengths and angles. As water molecules will be explicitly redocked as a component of the glide docking protocol, waters were removed from the protein during preprocessing. A constrained IMPACT Protein Refinement (IMPREF) minimization [32,42] was then conducted to a Root Mean Squared Deviation (RMSD) of 0.3 Angstroms.

A grid was generated using Trp193 as the center of a 20x20 Å box. Trp193 was selected as its role in binding the p22 peptide has been previously confirmed through point mutational analysis. Van der Waals radii were not

scaled in the receptor grid generation. Following the grid generation, the p22 peptide was removed from the binding groove. The Glide program generated a receptor grid and calculated energies of interaction of different atoms and groups in each cubic angstrom grids, scoring each individually.

The prepared protein was then imported into the Glide software for initial docking. Ligands were prepared by minimization using the Optimization Potential for Ligand Simulation 2005 (OPLS 2005) force field. The OPLS 2005 force field is a molecular mechanics force field including Lennard-Jones terms and Coulombic interactions. In creating the OPLS force field, Jorgensen, *et al.* found it unnecessary to include additional terms for hydrogen bonding and lone-pair interactions as the Lennard-Jones and Coulombic terms were found to be sufficiently descriptive [10]. To account for induced-fit, ligand Van der Waals radii were scaled to 0.8 of the initial value. The pH was set at 7.0 and all possible states for pH=6.8 to 7.2 were generated. To test for convergence over multiple runs, Glide SP and XP docks were repeated for the JM3-77C ligands.

Induced Fit Docking:

Induced fit docking was performed for JM3-77C, JM3-87B, & JM3-87C. This procedure allows for some receptor flexibility by allowing translation in bonds within 10 Å of the docked ligand. It is hypothesized that this is a better representation of a dynamic protein system than a rigid receptor. The ability of the induced fit method to account for these ligands by rank-order of potency was investigated.

Following rigid receptor docking, an induced fit docking was performed. The docking grid was centered on the lowest energy ligand pose obtained during Glide XP docking. A new grid was defined within 10 Å of the previously docked ligand. Minimized ligands were then subjected to an initial 'loose dock' whereby both the receptor and ligand Van der Waals radii were scaled by a factor of 0.50. Using the top 20 poses, the Prime homology modeling program was employed to optimize the geometry of the residues and side chains within 5.0 Angstroms of the ligand. Finally, an XP docking was performed whereby ligands were redocked into structures within 30.0 kcal/mole of the lowest energy structure. The top 50 of these structures were retained, although all poses above 0.5 kcal/mol were automatically eliminated. Finally, a rigid docking was performed using the new receptor geometry and scored with Glide XP.

Virtual Screening of Molecular Libraries:

Once favorable interactions were determined from docking studies, a hydrogen bond with Tryptophan 263 and the occupation of the proline rich region with a hydrophobic group, an effort was undertaken to leverage this information for the efficient screening of large libraries. A parameterized docking grid was calculated from the interaction of AS-99 with the binding groove, and the interactions were included as constraints. A minimized and conformationally prepared file containing structures of the approximately 118,000 compounds from the Chembridge molecular library was obtained from Pahk Thepchatri of the Emory Institute for Drug Discovery and Design (EIDD). This library of

compounds was docked to the $p22^{phox}$ binding site using Glide's High-Throughput Virtual Screening (HTVS) level of precision. The top 1,000 results obtained through the HTVS screen of the Chembridge library were then redocked using Glide Standard Precision (SP) and Glide Extra Precision (XP). 901 ligands, those generating poses below the 0.5 kcal/mol binding affinity energy threshold, were produced by the XP docking. As a negative binding affinity correlates with favorable ligand binding, a threshold of 0.5 kcal/mol was chosen as an arbitrary cutoff for rejecting ligand poses. Compounds identified through virtual screening were then clustered by Tantimoto similarity to select representative compounds from promising clusters, those possessing both Glide XP scores of at least 5 and favorable drug-like properties, for biological testing.

A standard precision rigid docking of Asinex's library of approximately 350,000 compounds was also performed. The use of a conformationally complete file containing all likely ligand orientations allowed for the use of the more efficient rigid docking. This removes the need for Glide to exhaustively sample ligand conformations, significantly reducing the computational expense for the virtual screening of large libraries. The top 1000 compounds will then be redocked with Glide XP and analyzed for clusters of structurally similar compounds. It is expected that compounds from promising clusters, will be procured for biological testing.

ROCS Searching:

The general biological principle driving ROCS, Rapid Overlay of Chemical Structures, searching is that similar molecules will have similar interactions [41]. In the case of ROCS, the 3-dimensional structure of the biologically active conformation, or the suspected biologically active conformation, is compared with the structures in a large library of molecules. For each overlay, the volume and electrostatic similarity are computed between the query and the candidate compound. The Tantimoto score, derived from the Jaccard Coefficient, is an indication of the similarity between two objects. The general form, for the Tantimoto between objects, A and B, with an overap of quality $S_{A,B}$ is shown below:

$$\textbf{Tantimoto}_{\mathbf{A,B}} = S_{A,B} / (S_{A,A} + S_{B,B} - S_{A,B}) \qquad [31, 36, 37]$$

When comparing two objects, this function will range between 0-1 where 1 indicates perfect shape similarity while 0 would indicate completely unrelatable molecules. The color Tantimoto is computed by comparing of atom types and electronegativities. To compare molecular shapes, the characteristic volume of the molecule must be calculated. This is accomplished by representing the molecular shape starting with atom-centered continuous Gaussians. Continuous functions describing molecular shape are then constructed from these Gaussians, which provides a significant simplification in the comparison among molecules as against treating the molecules as a set of discontinuous spheres represented by an atom. [31]

A ROCS search of the National Cancer Institute (NCI) molecular library was performed using the docked pose of JM3-77C as a template. The top 500 similar compounds were retained for further investigation. The top compounds were then docked using Glide SP. Pipeline Pilot software was employed for a clustering analysis of these compounds. Groups of compounds with a 2-Dimensional Tantimoto of greater than 0.4 were grouped together in an attempt to ascertain common structural features. A Tantimoto of 0.4 was chosen as this level of similarity allows for the grouping of molecules with similar core structures that still possess reasonably different side chains and substituent groups. This analysis was performed for both the top docking compounds and all of the ROCS hits.

Results and Discussion:

Model of Binding Orientation:

Glide docking studies were carried out on the active ligands JM3-77C, JM3-87B, & JM3 87 (*figure 10),* which differ in the ester's alkyl group, the smallest ligand AS-99 (*figure 12)* and the inactive ligands AS-108, AS-109 (*figure 13)*, TG4-140 (*figure 7)*, and TG4-225-2 (*figure 5)*. The corresponding poses demonstrated a common binding motif for active ligands with the carbonyl of the thiazole ring oriented down towards the amine of Trp263 and the sulfur or selenium facing towards the thiol ether of Met278. Hydrogen bonding with Ser279 was also observed in active compounds with a hydrogen bond acceptor in the *para* position of the benzene ring. This orientation compares favorably

with the interactions of $p22^{phox}$, the macromolecule being displaced by the inhibitory ligands. Docking of inactive compounds either failed to settle into an apparent favored orientation, as judged by the similarity of multiple poses, or were orientated in a manner “backwards” to that of the active compounds with the carbonyl orientated away from Trp263 and towards Met278.

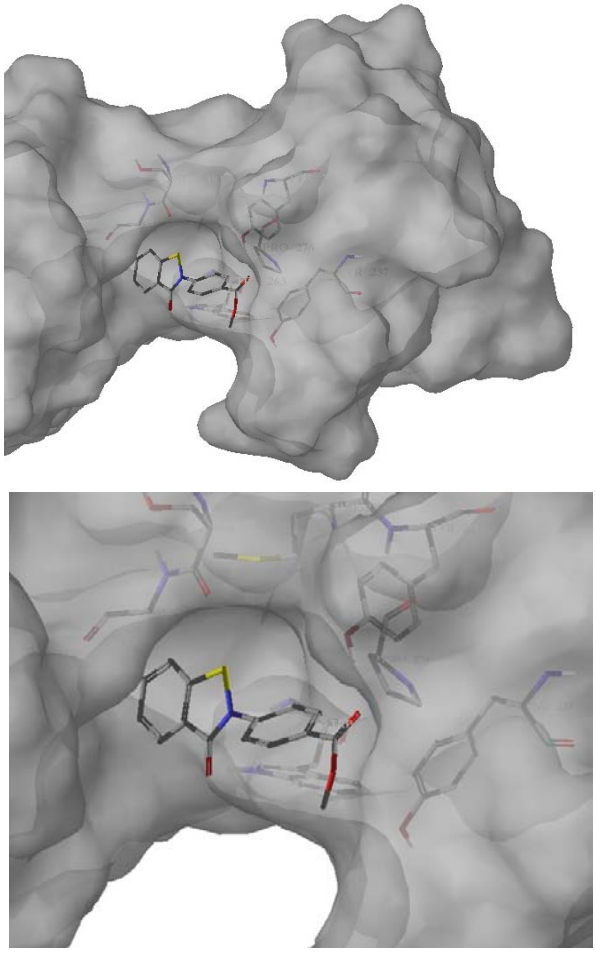

Figure 16: Representation of favored docking pose (JM3-77C docked in $p47^{phox}$)

JM3-53, *figure 17,* demonstrated a docked pose similar to the active ligands, although this only represented the top pose generated out of nine total

poses. Of the other generated poses, the representative pose shown in *figure 18* appeared to have the carbonyl facing away from Trp263.

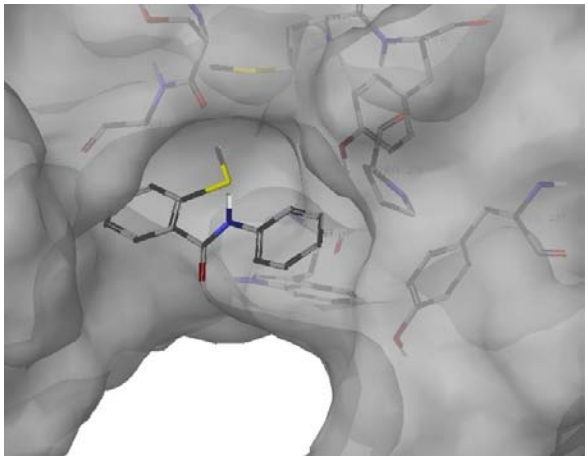

Figure 17: Top docked pose of JM3-53 in p47^{phox}

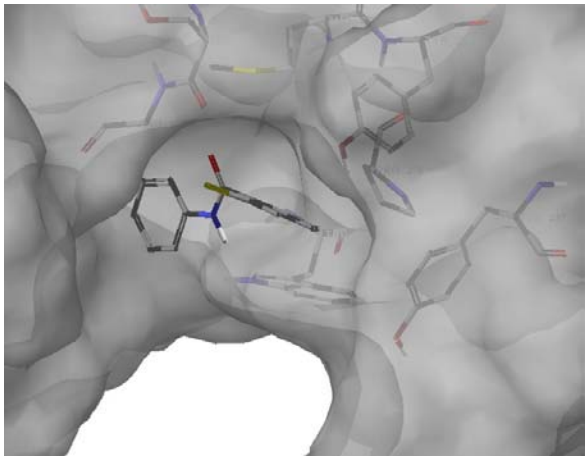

Figure 18: Second favored pose of JM3-53 in p47^{phox}

Docking of the oxazole containing compound, TG4 225-2, demonstrated two significant differences from docking of the compounds with known activity. As shown in *figure 19,* below, the generated poses involve a flat and rigid molecule. There was no rotation around the nitrogen-benzene bond, resulting in a perfectly flat molecule for most of the docked poses. Finally, in contrast to compounds

with known activity, the carbonyl of the oxazole ring is oriented away from the nitrogen of Trp263.

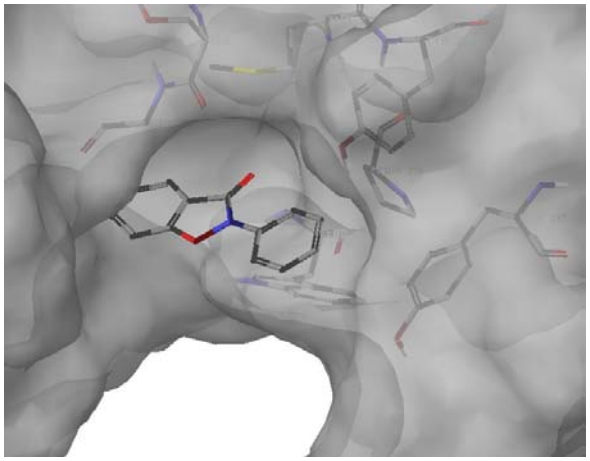

Figure 19: Docked pose of TG4 225-2 in p47^{phox}

Docking of TG4-140, in which the sulfur of the thiazole ring is replaced with carbon, does not generate any of the docking poses described above. As demonstrated in *figure 20,* below, it appears to fit poorly in the pocket and no discernable favored binding orientation is observed.

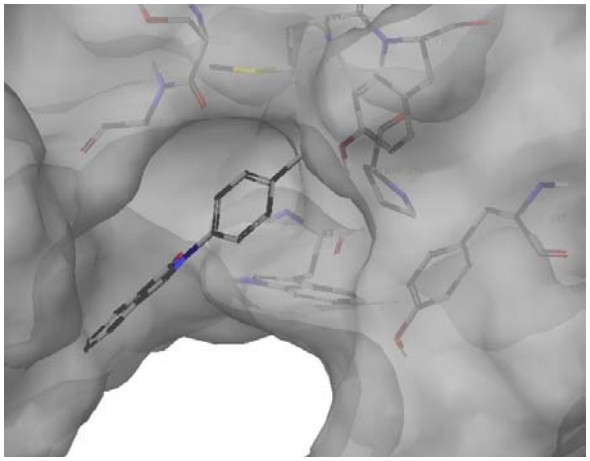

Figure 20: TG4-140 docked in p47^{phox}

The docking of JM3-77C generated four poses below the energy cutoff of 0.5 kcal/mol. Of these, three of four poses shown in the *figure 21* orientation directs the carbonyl toward Trp263's amine while the sulfur atom was oriented toward Met278. A hydrogen bond between the ester and Ser278 was also observed. Re-ranking the ligand poses using MMBGSA, which tends to favor hydrophobic interactions more than the Glide scoring function and allows for an extremely limited amount of receptor flexibility, delivered favorable orientations with the carbonyl facing downward. The three orientations with the carbonyl facing in the downward direction and the sulfur heteroatom facing Met278 showed a ΔG of binding of -23, -21, and -21 kcal/mol while the opposite orientation produced a score of -16 kcal/mol.

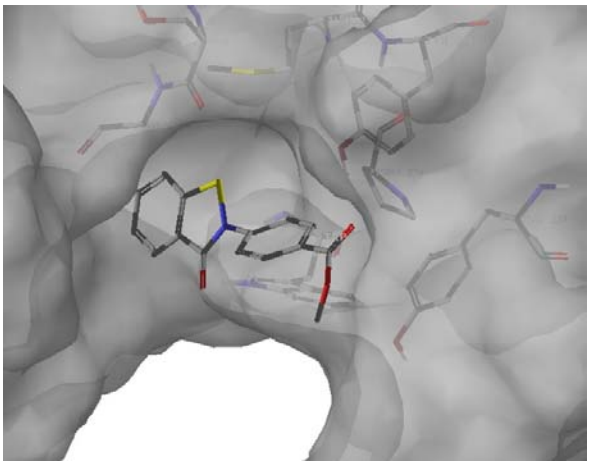

Figure 21: JM3-77C docked in p47^{phox}

An overlay of the docked pose of JM3-77C on the X-ray structure of the displaced peptide p22^{phox}, *figure 22,* shows occupation of similar geographic and electrostatic regions by both molecules. JM3-77C's benzene ring occupies the region containing the hydrophobic proline residues in the endogenous peptide.

The carbonyl of the thiazole ring is located in nearly the exact same location as the carbonyl from the inter-proline peptide bond. This similarity in the interactions supports the correctness of the Glide docking poses.

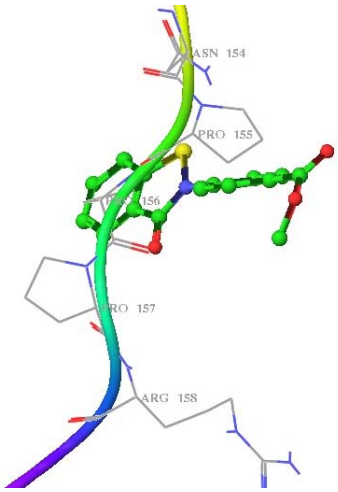

Figure 22: JM3-77C docked orientation shown with P22^{phox}

In two of four generated poses generated from docking JM3-87B, which contains a *tert*-butyl group in the ester moiety, produced similar results to JM3-77C (*figure 23*).

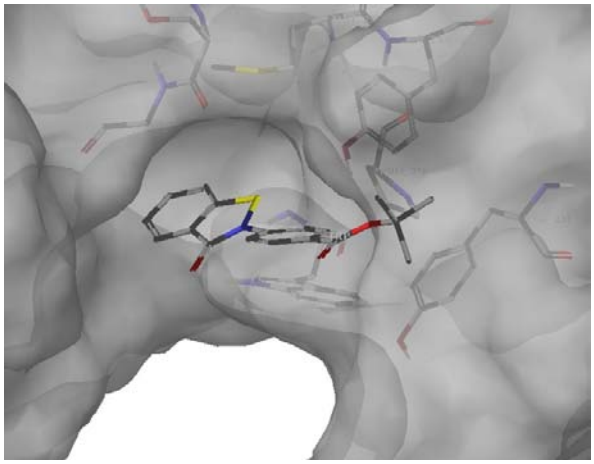

Figure 23: JM3-87B docked in p47^{phox}

A total of four poses were generated with JM3-87B. In contrast with JM3-77C, two of four poses show a downward facing carbonyl while the other poses include a carbonyl facing towards Met 278. Again, MM-GB/SA calculations for the carbonyl facing downwards both produced scores of -21 kcal/mol while the opposite orientation yielded ΔG binding scores of -18 and -17 kcal/mol. This is consistent with JM3-87C's reduced activity when compared with JM3-77C.

Glide docking of JM3-87C produced two ligand poses, shown in *figure 24*. Scoring these functions with MM-GB/SA produced scores of -30 for the ΔG of binding. These orientations differed slightly with the only difference being the orientation of the n-butyl chain.

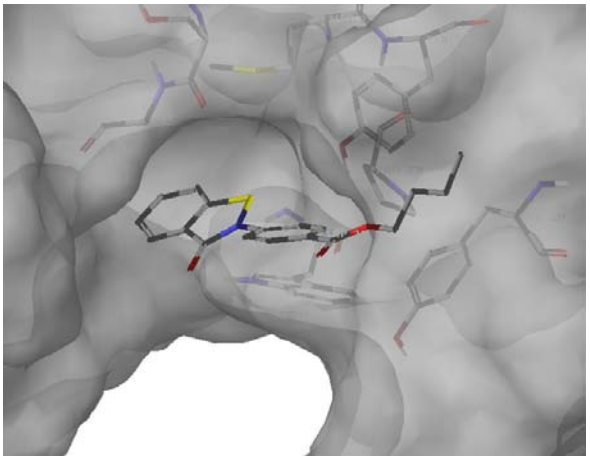

Figure 24: JM3-87C docked in p47^{phox}

Docking of AS-99, *figure 25,* a ligand with a known activity of 4.5 μM, generates 6 poses. Of these poses, 5 are of a ligand with the carbonyl in the downward position hydrogen bonding with Trp193. Similar to JM3-77C, 87B and 87C, these molecules also accept a hydrogen bond from Ser279.

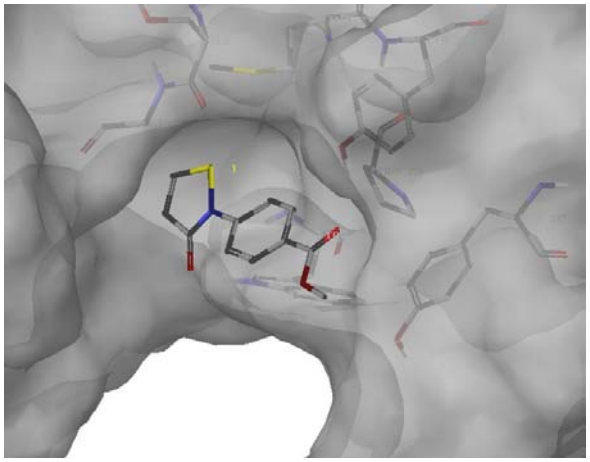

Figure 25: AS-99 docked in p47^{phox}

Similar to JM3-77C, a comparison of AS-99's docked pose with the endogenous p22^{phox} peptide reveals similar regional occupation and interactions. An overlay of both p22^{phox} and AS-109 is shown below in *figure 26*.

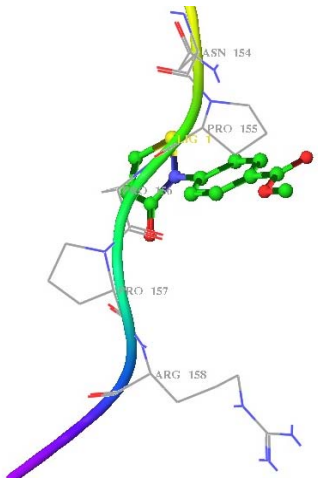

Figure 26: AS-99 docked orientation shown with p22^{phox}

At the same time, docking of AS-109, *figure 27,* a known inactive ligand, produced orientations favoring the orientation of the carbonyl facing towards Met278.

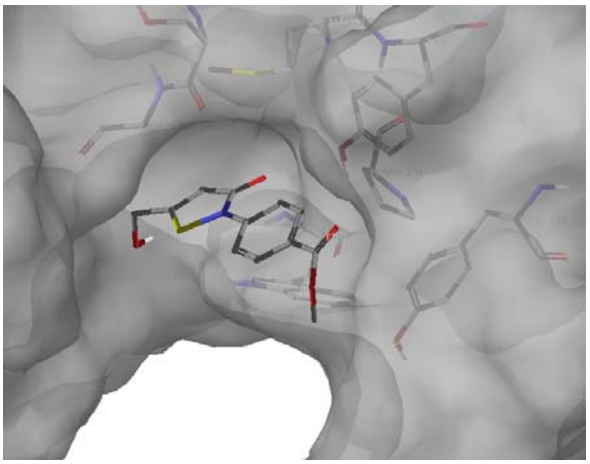

Figure 27: AS-109 docked in p47^{phox}

Figure 28 shows the conformation of the inactive compound AS-108, which does not appear to easily fit into the binding pocket. Likely due to its bulky nature, AS-

108 does not adapt any of the conformations seen with other ligands. This is in agreement with the observed lack of inhibitory activity against Nox2.

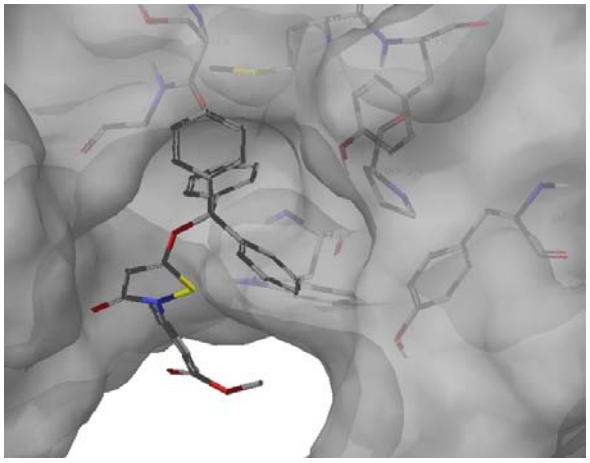

Figure 28: AS-108 docked in p47^{phox}

Glide docking poses and comparison of these poses with the bound endogenous p22^{phox} support the claim that active ligands bind in an orientation with the carbonyl of the central thiazole ring directed downwards allowing for hydrogen bonding with Trp263. The occupation of the p22^{phox} hydrophobic Pro206, Gly192, Asp206 and Met278 protein patch corresponding to the binding site previously occupied by the three p22^{phox} proline residues by a hydrophobic region of the ligand is also supported by this study. Though the docking grid was centered at Trp 193, a region corresponding to the PRR of p22^{phox}, and it may be suspected that this biased the docking results resulting in this region, the docking grid provided sufficient room to dock in other regions of the receptor grid. This information was used for a predictive study of possible AS-99 derivatives and to create constraints for a virtual screening of large molecular libraries.

Examination of the scoring functions in relation to the biological data with respect to JM3-77C, JM3-87B and JM3-87C shows that the Glide XP scores roughly correlates with experimentally determined binding energies. *Table 1* shows the Glide score for the top ranked pose of JM3-77C, JM3-87B and JM3-87C. As these ligands are structurally similar yet show significantly different activities, they represent ideal candidates for investigation of the scoring functions. As shown below, Glide XP scores correlate with the rank order of potency for the three ligands. This is not observed to be the case for induced fit docking and Glide SP. Assumptions made when docking, especially the scaling of Van der Waals radii to account for induce fit, reduce the ability for this program to adequately score molecules based on their rank-order of potency.

Table 1: IC_{50} values and docking scores

	JM3-77C	**JM3-87B**	**JM3-87C**
IC_{50} [11]	0.6μM	10 μM	7 μM
R-group	methyl	tert-butyl	n-butyl
Glide SP	-5.4	-5.0	-4.6
Glide XP	-4.5	-3.9	-3.9
Induced Fit Docking	-459	-459	-458

The docking conducted in this study demonstrated a pattern of poses correlating with ligand activity. As is shown with the poses generated by docking numerous active and inactive ligands, the active ligands generate poses with a “carbonyl-down” orientation and occupation of the region surrounded by Pro 206,

Gly 192, Asp 206 and Met 278 with a hydrophobic group. Though Glide scoring was not shown to directly correlate with the rank-order of potency, a reasonable model of a favorable interaction with the ligand was generated in this work. Though this model accounts for the properties of many active and inactive ligands, the ultimate value of this model is its ability to make predictions and aid in the drug discovery process. The docking orientations can be examined to search for ways to a scaffold's structure or functionality to optimize its binding properties. Potential new scaffold derivatives can be docked and analyzed for favorable interactions prior to synthesis, inducing a significant efficiency into the process of optimizing compounds for activity. Finally, this model can be used for the screening of large molecular libraries for possible active ligands. The constraints derived as from this understanding of the favored docking modes, requiring molecules to have the ability to fit the model's motif for active ligands, can serve as a further enrichment for the virtual screening of molecular libraries. This both reduces the time necessary for screening large libraries and increases the probability of including active compounds among the top docking poses. This model can significantly economize and streamline the process of discovering and optimizing novel Nox2 inhibitors.

Predictive Studies of AS-99 Derivatives:

Initially, possible derivatives of the AS-109 scaffold, ***figure 29,*** were investigated for likely activity. Tested substituents were chosen for their perceived ability, based on docked poses of AS-99, to either act as a hydrogen

bond acceptor or favorably occupy a hydrophobic region. Fluorinated compounds were studied as fluorine is approximately identical in volume to hydrogen and can act as a hydrogen bond acceptor. A proline mimetic substituent was chosen due to presence of this residue in the endogenous $p22^{phox}$. Finally, the Diels Alder adducts of furan and cyclopentadiene with AS-99 were studied at the suggestion of Aiming Sun due to the relative simplicity of this reaction.

1 **2** **3**

R_1= Me, Et, MeF, EtF, OMe, OEt, iPr, Ph
R_2= Me, Et, MeF, EtF, OMe, Ph
R_3= Me, Et

4 **5**

Figure 29: AS-99 scaffold derivatives for predictive studies

From these studies, it was found that substitution at the R_2 position in **1** produced less favorable ligand orientations relative to the parent scaffold, AS-99 while substitution at the R_1 position showed more favorable docking poses. Substitution at the R_1 position

tended to occupy a hydrophobic pocket to push the molecule slightly out of the docking pocket in a manner that improved the hydrogen bonding interaction with both Trp263 and Ser279. This is shown in *figure 31* with the ethyl substituted derivative.

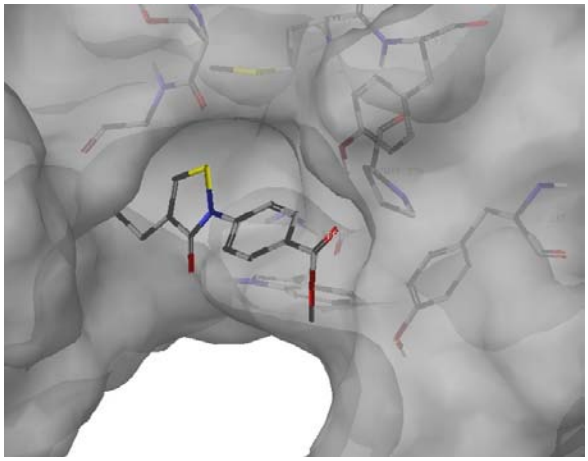

Figure 30: Ethyl substitution at R_1 in 1

Docking poses for generated from docking both the proline mimetic **4**, *figure 31*, and the furan Diels-Alder adduct **2**,*figure 32,* show an ability for the substituent groups to both accept a hydrogen bond from Trp263 and improve the hydrogen bonding interaction with Ser279. It is believed that these ethyl substituted, proline-mimetic **4**, and diels-alder adducts **2** should show a significant improvement in activity over the parent scaffold, AS-99.

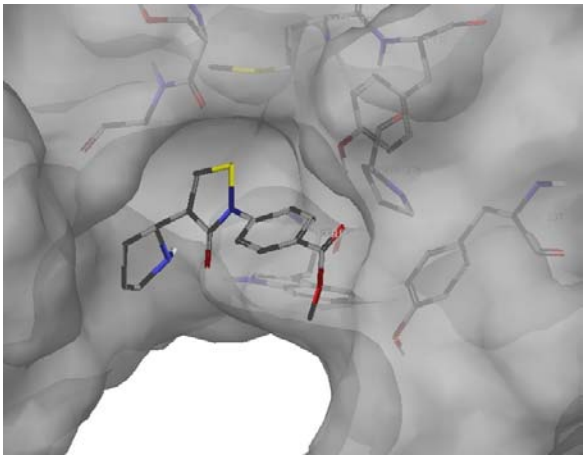

Figure 31: Proline mimetic at R_1 in number 4

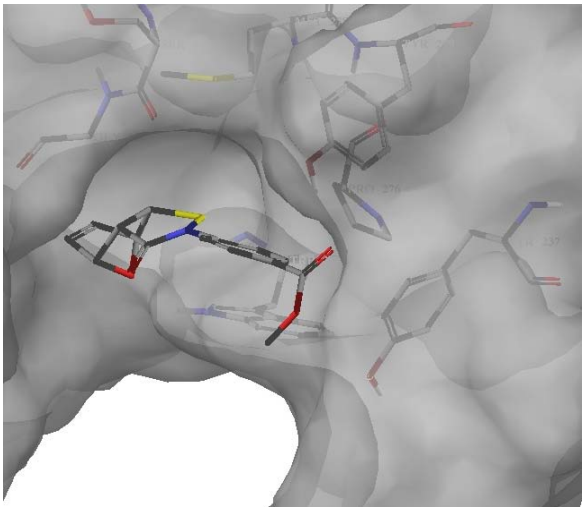

Figure 32*: Diels-Alder adduct in number 2*

Molecular Library Screening:

Chembridge and Asinex libraries were screened using constraints generated from the binding model generated above. Constraints requiring the ability to hydrogen bond with Trp263 and the occupation of a hydrophobic region

corresponding to the olefin bond of AS-99 were generated and utilized for database searching. All screening protocols were set to return a maximum of 1,000 hits. A Glide SP screening of the Asinex library has been conducted, though the 1,000 returned compounds currently await further analysis. The initial High Throughput Virtual Screening (HTVS) of the Chembridge library produced 1,000 compounds. XP redocking produced 901 compounds below the 0.5 kcal/mol energy threshold.

XP re-docking and MM-GB/SA scoring of the top 1,000 compounds obtained through a High Throughput Virtual Screening (HTVS) of the Chembridge library revealed a number of promising leads. The results from this screen were clustered by 2-D Tantimoto similarity prior for further analysis. Compounds from the Glide XP re-dock were grouped into 176 clusters, with molecules in each group all having a 2-D Tantimoto similarity score of greater than 0.6. Representative compounds from promising clusters, those exhibiting both good docking scores and favorable drug-like structures are shown below in *figure 33.*

Figure 33: ***Representative hits from virtual screening of Chembridge Library***

Common features among many of these compounds include the presence of a mercaptoamine functionality or acetamide functionality, amine containing heterocycles and aromatic substituents. The mercaptoamine compounds exhibit the highest docking scores, typically -7 to -8 kcal/mole in Glide XP scoring and -30 to 35 kcal/mol in MM-GB/SA scoring, though all of the top groups exhibited Glide XP scores of -6 or greater and MM-GB/SA ΔG_{bind} of at least -30 kcal/mol, which compares favorably to the current ligands. It is recommended that compounds from the top 50 scoring clusters be procured and submitted for testing using the FP assay. Compounds exhibiting activity can then be further optimized through synthetic derivatization and screening of analogous

compounds to develop a lead compound from a new and scaffold for drug-development.

ROCS Searching:

Rapid Overlay of Chemical Structures (ROCS) searching the NCI database using the structure of JM3-77C, *figure 10,* as the parent structure. 500 ROCS hits were returned from this search. Representative molecules from screening results are shown below in *figure 34.* As seen below, the molecules returned from this search showed substantial similarity to the current thiazole scaffold, sugar derivatives and quinones. For reasons including the EIDD's previous experience with quinines, the large amount of prior art available for these molecules these molecules' ability to act as an oxidizing agent *in-vivo* it was decided not to further pursue these compounds for future development. Sugar derivatives were not pursued further because of the difficulty and expense of synthetically optimizing this class of scaffolds. Though it is possible that ROCS searching may have led to a viable alternative scaffold, it was ultimately decided focus efforts towards methods that did not rely on and tend to return results similar to the problematic thiazol scaffold.

Figure 34: Representative hits from ROCS searching

Conclusion:

The successful inhibition of the NADPH Oxidase Nox2 remains a difficult and desirable target for medicinal chemistry. Selectively targeting Nox2 and its homologues may well allow for a significant reduction in the production of harmful ROS that is associated with disease states affecting millions. The enzyme's effects are wide-ranging from acute disease states, such as ischemic stroke, to the prevention of chronic diseases, such as Type II diabetes and cardiovascular disease. The development of a therapeutic selectively inhibiting isoforms of NADPH Oxidases could very well represent a significant chemical tool for use in preventative medicine that would allow physicians to halt the progression of otherwise debilitating and dangerous diseases. This work utilized Glide docking to investigate the binding Nox blockers and the Nox2 subunit $p47^{phox}$. ROCS

searching was employed in an attempt to search for an alternate viable lead drug.

Investigation of ligand binding with Glide docking generated a model for a likely mode of binding that is in agreement with experimentally determined potencies. This model was utilized for the virtual screening of large molecular libraries and the refinement of virtual screening results. Biological results from these screens and derivatives of AS-99 should provide some qualification of the model's validity and correctness. Upon validation, this model could be used for an efficient screening of all known drug-like compounds against the $p47^{phox}$ receptor in search of a viable lead ligand for the therapeutic inhibition of Nox2.

Although this model provides a potentially predictive tool that may allow for the selection of an alternative scaffold a number of issues remain in the path to discovering a viable Nox2 inhibitor drug. As the receptor is a site of protein-protein interaction, a target that represents one of the most difficult classes of drug target, it remains to be seen if a potent small-molecule inhibitor for this site is possible. Though it is hoped that by using a ligand with sufficient selectivity to block individual Nox isoforms and thereby target specific regions and disease major side-effects can be avoided, the undesired physiological results from a successful inhibition of Nox2 remain a significant concern. Among the main concerns is that, due to the central role of Nox2 in immune defense, an inhibitor could degrade the body's ability to fight off and prevent infections. This is especially relevant considering the potential and long-term uses, especially for preventative indications. Although Nox2 inhibitors show great promise as a

prophylactic for many serious and debilitating diseases, success in use for a long-term indication will require a near-perfect safety profile. Despite these challenges Nox2 remains a desirable drug target and this work, upon proper validation through biological screening of virtual hits, may provide a tool to aid in discovering and developing a Nox2 inhibitor.

References:

1. Babior, Bernard M. Phagocytes and Oxidative Stress *Physiology in Medicine* **2000,** 109, 34-44
2. Lambeth, D.; Krause, K.; Clark, R. NOX enzymes as novel targets for drug development *Semin Immunopathol* **2008,** 30, 339-363
3. Geiszt, M.; Witta, J.; Baffi, J.; Lekstrom, K. & Leto, T. Dual Oxidases represent novel hydrogen peroxide sources supporting mucosal surface host defense. *FASEB J.* **2003,** 17, 1502-1504
4. Lambeth, D. NOX Enzymes and the Biology of Reactive Oxygen *Nature Reviews, Immunology* **2004,** 4, 181-189
5. Groemping, Y; Lapouge, K.; Smerdon, S.; Rittinger, K. Moleculare Basis of Phosphorylation-Induced Activation of the NADPH Oxidase *Cell* **2003** 113, 343-355
6. Friesner; Banks; Murphy; Halgren; Klicic; Mainz; Repasky; Knoll; Shelly; Perry; Shaw; Francis; Shenkin Glide: A new Approach for Rapid, Accurate Docking and Scoring. 1. Method and Assessment of Docking Accuracy *Journal of Medicinal Chemistry* **2004,** 47, 1739-1749
7. Halgren, Thomas A.; Murphy, Robert B.; Friesner, Richard A.; Beard, Hege S.; Frye, Leah L.; Pollard, Thomas W.; Banks, Jay L. Glide: A New Approach for Rapid, Accurate Docking and Scoring. 2. Enrichment Factors in Database Searching *Journal of Medicinal Chemistry* **2004,** 47, 1750-1759
8. Eldridge, Matthew D.; Murray, Christopher W.; Auton, Timothy R.; Paolini, Gaia V.; Mee, Roger P. Empirical scoring functions: I. The development of

a fast empirical scoring function to estimate the binding affinity of ligands in receptor complexes. *Journal of Computer-Aided Molecular Design* **1997,** 11, 425-445

9. Salam, Noeris K.; Nuti, Roberto; Sherman, Woody Novel Method for Generating Structure-Based Pharmacophore Using Energetic Analysis. *J. Chem. Inf. Model.* **2009** 40(10), 2356-2368
10. Jorgensen, William L. & Tirado-Rives, Julian The OPLS Potential Functions for Proteins. Energy Minimizations for Crystals of Cyclic Peptides and Crambin *Journal of the American Chemical Society* **1988,** 110(6) 1657-1671
11. Frisner, R.; Murphy, R.; Repasky, M.; Frye, L.; Greenwood, J.; Halgren, T.; Sanschagrin, P.; Mainz, D. Extra Precision Glide: Docking and Scoring Incorperating a Model of Hydrophobic Enclosure for Protein-Ligand Complexes *J. Med. Chem.* **2006,** 49, 6177-6196
12. Lambeth, Dave; Smith, Susan; Unpublished Results
13. Jaquet, Vincent; Scapazzo, Leonardo; Clark, Robert A.; Krause, Karl-Heinz; Lambeth, David J., Small-Molecule NOX Inhibitors: ROS-Generating NADPH Oxidases as Therapeutic Targets, *Antioxidants & Redox Signaling,* **2009,** 11(10), 2535-2551
14. Berendes, H; Bridges R; Good R A fatal granulomatosus of childhood: the clinical study of a new syndrome *Minnesota Medicine* **1957** 40(5), 309-12
15. National Institute of Diabetes and Digestive and Kidney Diseases. National Diabetes Statistics, 2007 fact sheet. Bethesda, MD: U.S.

Department of Health and Human Services, National Institutes of Health, 2008.

16. Li, Jian-Mei & Shah, Ajay M. Mechanism of Endothelial Cell NADPH Oxidase Activation by Angiotension II. Role of the $p47^{phox}$ subunit. *The Journal of Biochemistry and Molecular Biology* **2003,** 278(14), 12094-12100
17. Ebselen in acute ischemic stroke: A placebo-controlled, double-blinded clinical trial *International Joint Conference on Stroke and Cerebral Circulation Orlando, FL Number 23* **1998,** 29(1) 269-335
18. Yamaguchi, T.; Sano, K.; Takakura, K.; Saito, I.; Shinohara, Y.; Asano, T.; Yasuhara, H. Ebselen in Acuta Ischemic Stroke: A Plaebo-Controlled, Double-blind Clinical Trial *Stroke* **1998,** 29, 12-17
19. Imai, H.; Masayasu, H.; Dewar, D.; Graham, D.I.; Macrae, I.M. Ebselen Protects Both Gray and White Matter in a Rodent Model of Focal Cerebral Ischema, *Stroke* **2001,** 32, 2149-2154
20. Lambeth, D. Nox Enzymes, ROS, and chronic disease: An example of antagonistic pleiotropy, *Free Radical Biology & Medicine,* **2007**, 43:332-347
21. Segal, A. W. The NADPH oxidase and chronic granulomatis disease. *Molecular Medicine Today* **1996** 2, 129-135
22. Ullrich, V.; Weber, P.; Meisch, F.; von Appen, Frank Ebselen-Binding Equilibria Between Plasma and Target Proteins, *Biochemical Pharmacology* **1996** 52, 15-19

23. Novak, W.; Hongming, W.; Krilov, G.; Role of protein flexibility in the design of Bcl-X_L targeting agents: insight from molecular dynamics, *Journal of Computer Aided Molecular Design* **2009**, 23, 49-61
24. Eyrish, S.; Helms, V., What induced pocket openings on protein surface patches involved in protein-protein interactions? *Journal of Computer Aided Molecular Design* **2009** 23:73-86
25. Eyrish, S.; Helms, V., Transient Pockets on Protein Surfaces Involved in Protein-Protein Interaction *Journal of Computer Aided Molecular Design* **2007** 50:3457-3464
26. Berg, Thomas, Modulation of Protein-Protein Interactions with Small Organic Molecules *Angewandte Chemie* **2003** 42, 2462-2481
27. Yin, H.; Hamilton, A., Strategies for Targeting Protein-Protein Interactions With Synthetic Agents *Angewandte Chemie* **2005** 44, 4130-4163
28. El-Benna, J.; Dang, P.; Gougerot-Pocidalo, M.; Marie, J.; Braut-Boucher, F. p47phox, the phagocyte NADPH oxidase/Nox2 organizer: structure, phosphorylation and implication in disease, *Experimental and Molecular Medicine* **2009**, 41(4), 217-225
29. Kessl, J.; Eidahl, J.; Shkriabai, N.; Zhao, Z. An Allosteric Mechanism for Inhibiting HIV-1 Integrase with a Small Molecule, *Molecular Pharmacology* **2009**, 76, 824-832
30. Ago, T.; Nunoi, H.; Ito, T.; Sumimoto, H. Mechanism for Phosphorylation-induced Activation of the Phagocyte NADPH Oxidase Protein $p47^{phox}$ *The Journal of Biological Chemistry* **1999,** 274(47), 33644-33653

31. Rush, T.; Grant, J.; Mosyak, L.; Nicholls, A. A Shape-Based 3-D Scaffold Hopping Method and Its Application to a Bacterial Protein-Protein Interaction, *Journal of Medicinal Chemistry,* **2005** 48, 1489-1495
32. Schrodinger L.L.C., New York, New York
33. Zhou, Z.; Felts, A.; Friesner, R.; Levy, R. Comparitive Performance of Several Flexible Docking Programs and Scoring Functions: Enrichment Studies for a Diverse Set of Pharmaceutically Relevant Targets *Journal of Chemical Information and Modeling* **2007,** 47(4), 1599-1608
34. Lipinski, C.; Lombardo, F.; Dominy, B.; Feeney, P. Experimental and computational approaches to estimate solubility and permeability in drug discovery and development settings *Advanced Drug Delivery Reviews* **1997**, 23, 3-23
35. Lipinski, Christopher A. Drug-like properties and the causes of poor solubility and poor permeability *Journal of Pharmacological and Toxicological Methods* **2000**, 44, 235-249
36. Jaccard, P. Étude comparative de la distribution florale dans une portion des Alpes et des Jura *Bulletin del la Société Vaudoise des Sciences Naturelles*, **1901** 37, 547-579.
37. Hamers, L.; Hemeryck, Y.; Herweyers, G.; Janssen, M.; Keters, H.; Rousseau, R.; Vanhoutte, A. Similarity Measures in Scientific Research: The Jaccard Index Versus Salton's Consine Formula *Information Processing & Management* 1989 25(3), 315-318

38. Kobayashi, S.; Murayama, S.; Takanashi, S.; Takahashi, K.; Miyatsuka, S.; Fujita, T.; Ichinoe, S.; Koike, Y.; Kohagizawa, T.; Mori, H.; Deguchi, Y.; Higuchi, K.; Wakasugi, H.; Sato, T.; Wada, Y.; Nagata, M.; Okabe, N.; Tatsuzawa, O. Clinical features and prognoses of 23 patients with chronic granulomatous disease followed for 21 years by a single hospital in Japan *European Journal of Pediatrics,* **2008,** 167, 1389-1394
39. Madamanchi, N.; Runge, M NADPH oxidases and atherosclerosis: unraveling the details *American Journal of Physiology- Heart and Circulatory Physiology* **2010,** 298, H1-H2
40. Berman, H.; Bhat, T.; Bourne, P.; Feng, Z.; Gilliland, G.; Weissig, H.; Westbrook, J. The protein Data Bank and the challenge of structural genomics *Nature Structural Biology* **2000**, 11, 157-959
41. OpenEye Scientific Software, Santa Fe, NM
42. Banks *et al.* Integrated Modeling Program, Applied Chemical Theory (IMPACT) *Journal of Computational Chemistry* **2005,** 26(16), 1752-1780
43. Fenn, J.; Mann, M.; Meng, C.; Wong, S.; Whithouse, C. Electrospray ionization for mass spectrometry of large biomolecules *Science* **1989,** 246(4926) 64-71
44. Guimaraes, C.; Mathiowetz, A. Addressing Limitations with the MM-GB/SA Scoring Procedure using the WaterMap Method and Free Energy Pertubation Calculations *Journal of Chemical Information and Modeling (online)* **2010,** 10.1021/ci900497d